BROWN, R, and CHANSON, H. (2013). "Turbulence and Suspended Sediment Measurements in an Urban Environment during the Brisbane River Flood of January 2011." *Journal of Hydraulic Engineering*, ASCE, Vol. 139, No. 2, pp. 244-252 (DOI: 10.1061/(ASCE)HY.1943-7900.0000666) (ISSN 0733-9429).

TURBULENCE AND SUSPENDED SEDIMENT MEASUREMENTS IN AN URBAN ENVIRONMENT DURING THE BRISBANE RIVER FLOOD OF JANUARY 2011

Richard Brown ([1]) and Hubert Chanson ([2]) ([*])

([1]) Associate Professor, Queensland University of Technology, Faculty of Built Environment and Engineering, Brisbane QLD 4000, Australia

([2]) Professor in Hydraulic Engineering, The University of Queensland, School of Civil Engineering, Brisbane QLD 4072, Australia, Ph.: (61 7) 3365 4163, Fax: (61 7) 3365 4599, E-mail: h.chanson@uq.edu.au

([*]) Corresponding author

Abstract: In urbanised areas, the flood flows constitute a hazard to populations and infrastructure as illustrated during major floods in 2011. During the 2011 Brisbane River flood, some turbulent velocity data were collected using acoustic Doppler velocimetry in an inundated street. The field deployment showed some unusual features of flood flow in the urban environment. That is, the water elevations and velocities fluctuated with distinctive periods between 50 and 100 s linked with some local topographic effects. The instantaneous velocity data were analysed using a triple decomposition. The velocity fluctuations included a large energy component in the slow fluctuation range, while the turbulent motion components were much smaller. The suspended sediment data showed some significant longitudinal flux. Altogether the results highlighted that the triple decomposition approach originally developed for period flows is well suited to complicated flows in an inundated urban environment.

Keywords: Flood plain, urban environment, turbulence measurements, triple decomposition, suspended sediment concentration SSC, water body resonance, Brisbane River.

INTRODUCTION

The flood flows in urbanised areas constitute a hazard to the populations and infrastructure. Some recent catastrophes included the inundations of Vaison-la-Romaine (France) in 1992 and Nîmes (France) in 1998, the flooding of New Orleans (USA) in 2005, the floods in Queensland (Australia) during the summer 2010-2011, and the Mississippi River flood (USA) in spring 2011. Flood flows in urban environments have only been studied relatively recently despite many centuries of flood events. Some researchers mentioned the storage effect in urban areas (Solo-Gabriele and Perkins 1997, Velickovic et al. 2011). Other studies looked into the flow patterns and redistribution in streets during storm events and the implication in terms of flood modelling (Bates et al. 2004, Nania et al. 2004, Werner et al. 2005, Velickovic et al. 2011). A number of studies looked at the impact of floods on structures and buildings (Thieken et al. 2005). Some considered the potential impact of flowing waters on pedestrians (Asai et al. 2010, Ishigaki et al. 2003). However, to date, there are limited field observations as well as no basic methodology to analyse turbulent velocity measurements collected in a complex urban environment.

In the present study, some turbulent velocity and suspended sediment concentration measurements were conducted at relatively high-frequency (50 Hz) in a flooded street during the 12-13 January 2011 flood of the Brisbane River (Australia) (Fig. 1 & 2). The results highlighted some difficulties to interpret the raw data without proper decomposition. It is the aim of the present work to present an innovative characterisation of turbulence and sediment flux in the inundated urban environment. The field investigation and instrumentation are described in the next section. The main results are presented in the following sections. It must be stressed that the study is a detailed analysis of point measurements in an inundated urban setting rather than a detailed study of the whole flood event.

FIELD INVESTIGATION AND INSTRUMENTATION

INVESTIGATION SITE

Located along the Brisbane River, the central business district (CBD) of the City of Brisbane is about 25 km upstream of the river mouth (Fig. 1A) and the catchment area is 13,500 km^2 (Institution of Engineers, Australia 1974). Following some heavy rainfall in the catchment during early January 2011, the Brisbane River water level rose rapidly on 11 and 12 January 2011 (Chanson 2011). The city of Brisbane was flooded from 11 to 14 January with the flood waters peaking on 13 January 2011 early morning in the city. Figure 3A shows the flood hydrograph of the Brisbane River at the City Gauge (location shown in Fig. 1A). The data are compared with the predicted tidal level at the same location; both data and predictions are measured above the Australian Height Datum (AHD). At the peak of the flood, the estimated river discharge was in excess of 9,000 to 10,000 m^3/s in the city reach (Malone, T. 2011, *Pers. Comm*) and the local friction slope was about 1×10^{-4} (Brown et al. 2011). The hydrograph data of the Brisbane River in the city (Fig. 3) may be compared to the peak levels of 5.45 m AHD in 1974 and 8.35 m AHD in 1893, while the city experienced 6 major floods with higher water levels in the last 180 years (Chanson 2011).

Some turbulent velocity measurements were performed along Gardens Point Road in the QUT Gardens Point campus below C Block building between 12 and 14 January 2011. The site was located between Gardens Point Road and the ground floor car park (Fig. 1 & 2). Figure 1 shows some aerial views prior to the flood with the red arrow pointing to the sampling site. Figure 2A presents a photograph taken during the flood with the acoustic Doppler velocimeter (ADV) locations. Figure 2B details the ground floor car park of C Block building and Figure 2C shows a cross-sectional survey looking downstream. Further details and photographs were reported by Brown et al. (2011).

INSTRUMENTATION

The free surface elevations were recorded manually using a measuring tape with reference to landmarks which were surveyed after the flood. The turbulent velocities were measured with a Sontek^{TM} microADV (16 MHz, serial A843F) equipped with a 3D side-looking head. For a series of data (Table 1, series 1), the unit was placed horizontally with the head pointing downwards. After the ADV was dislodged by a timber log, the unit was re-positioned vertically and attached to a hand rail (location B, series 2 & 3). During each series, the ADV was sampled continuously at 50 Hz (Table 1, column 3). The ADV unit was equipped with a pressure sensor which was underwater and gave some instantaneous water elevation data during the first series of data (series 1). During the other series, the pressure sensor was out of the water.

All the ADV data underwent a thorough post-processing procedure to eliminate any erroneous or corrupted data from the data sets to be analysed. The post processing included the removal of communication errors, the removal of average signal to noise ratio (SNR) data less than 5 dB and the removal of average correlation values less than 60% (McLelland and Nicholas 2000). In addition, the phase-space thresholding technique developed by Goring and Nikora (2002) and extended by Wahl (2003) was applied to remove spurious points.

Some sediment material was collected on 13 and 14 January 2011 along Gardens Point Road. The soil samples consisted of fine mud ($d_{50} \approx 26$ μm). The calibration of the ADV unit in terms of suspended sediment concentration (SSC) was accomplished by measuring the signal amplitude of known, artificially produced concentrations of material obtained from the bed material sample, diluted in tap water and thoroughly mixed. All the experiments were conducted on 18 January 2011 with the same microADV (serial A843F) using the same settings as for the field observations on 12-14 January 2011. The results indicated a decreasing signal amplitude with increasing SSC, linked with some signal attenuation previously observed in cohesive materials at high concentrations (Fig. 4) (Ha et al. 2009, Chanson et al. 2012).

REMARKS

Two ADV settings were used (Table 1, column 4). The lower velocity range was selected for the last two samplings after the flood started to recede, and slower velocities were observed.

During the field deployment, a number of problems were experienced. During the first series, the ADV was dislodged by the impact of a timber log and "wheelie" bin. The ADV unit was repositioned to a nearby handrail. During the second series, the ADV unit had to be stopped because the generator was required to assist flood victims whose homes were without electricity. A smaller generator was installed and the ADV was restarted two hours later. The third series ended when the flood waters receded and the upper ADV receiver came to be out of the water.

BASIC OBSERVATIONS

During the rising stage of the Brisbane River flood on 11 and 12 January, the river swelled and inundated Gardens Point Road (Fig. 2). The left flood plain included some car parks located beneath Captain Cook Bridge (Fig. 2A, left), Gardens Point Road and car parks beneath a number of buildings (Fig. 2C). Although a relatively fast flow motion was observed along Gardens Point Road, visual and photographic observations indicated that the free-surface flow in Gardens Point Road was subcritical on 12 and 13 January 2011. During the flood, the authors went into the C Block car park and Gardens Point Road to install the ADV system and later to re-locate the unit. They observed some slow fluctuations of water level and felt some water surges with periods of about one minute. These slow fluctuations were associated with changes in water elevations of up to 0.1 to 0.2 m. On 13 January night, the flood waters receded leaving a 2-10 cm thick layer of soft mud.

The water depths, and corresponding elevations, were recorded manually on three occasions (Fig. 3, filled hexagons).The manual water depth records were 0.89 m, 0.67 m and 0.26 m at t = 72,000 s, 127,800 s and 145,800 s respectively. Further the pressure head above the ADV pressure sensor was recorded continuously during the first data series. The observations are reported in Figure 3 together with the Brisbane River levels recorded at the City Gauge located 1.55 km downstream. Both the manual observations and pressure head fluctuations showed some trends that were close to the Brisbane River water level record at the City Gauge (Fig. 3B).

The pressure sensor readings highlighted some large fluctuations of the water level around its mean trend (black thick line, Fig. 3B). The measurements of water level h, longitudinal velocity V_x and velocity flux $q = V_x h$ showed some low-frequency oscillations with periods of about 50 to 100 s close to the visual observations. A spectral analysis of the data was performed. Although not shown, the lower frequency limit of the -5/3 slope inertial range was typically in the range of 0.5 to 2 Hz. Figure 5 shows some frequency analyses of water level and velocity fluctuations during the data series 1. Note that the data sets were truncated at 0.5 Hz for clarity. The results highlighted a peak in power spectrum density (PSD) functions for periods about 50 to 100 s (about 60 s for the data series 1 in Fig. 5) together with higher energy density levels around the characteristic peak(s). For the water level, velocity flux, velocity components, suspended sediment concentration (SSC) and suspended sediment flux ($q_s = V_x SSC$), the dominant slow fluctuation periods are summarised in Table 2. The results highlighted the presence of slow fluctuations with characteristic periods between 50 and 100 s for all data series in terms of water depth, velocity flux and velocity components (Table 2). The dominant period increased with decreasing water depths. Some simple hydraulic calculations showed that it was close to the first mode of natural sloshing resonance linked with the C Block building length (L = 70.2 m) (Brown et al. 2011).

DISCUSSION

At the sampling location, the flow motion was subcritical throughout the study. It is believed however that the flow in the car park (C Block level 1) was affected by choking in the constriction induced by two stairwells located upstream (Fig. 2B). The gap between stairwells was 10 m compared to the C Block car park width of 33.6 m. Based upon the observed water depth and mean longitudinal velocity data, some basic hydraulic calculations show that the constricted flow could reach transcritical flow conditions between the stairwells. For a given specific energy and discharge, choking may occur when the channel constriction is too narrow, and additional specific energy is required to maintain the flow rate (Henderson 1966, Montes 1988). Some energy considerations show that the total head loss in the stairwell constriction could be as large as 0.05 to 0.15 m during the flood flow.

When the flow in the stairwell constriction reached transcritical conditions, choking would take place, and additional energy would be required to maintain the flow rate inducing additional head losses. The energy losses in the constriction could become substantially larger than the rate of energy loss of the main flow in Gardens Point Road, and the inundation flow would redirect around the stairwells to achieve a minimum energy path. The pattern would be responsible for some flow oscillation in the surroundings of the stairwells with a period close to the natural sloshing period of the building car park. In summary, it is believed that the excitation source of the observed slow fluctuations was some choking in the flow constriction between stairwells (Fig. 2B) and associated energy losses.

FLOW PARAMETERISATION

In the above paragraph, some slow-frequency fluctuations in both water elevations and velocity components were observed and the velocity field exhibited a fluctuating behaviour with periods between 50 and 100 s (Table 2). A triple decomposition of the instantaneous velocity data was performed. The technique was previously applied to periodic turbulent flows and riverine flows with large coherent structures (Hussain and Reynolds 1972, Fox et al. 2005, Yossef and de Vriend 2011).

In the present study, the instantaneous velocity time-series may be represented as a superposition of three components:

$$V = \langle V \rangle + [V] + v \qquad (1)$$

where V is the instantaneous velocity, <V> is the mean velocity contribution, [V] is the slow fluctuating component of the velocity and v corresponds to the turbulent motion. Herein <V> is the low-pass filtered data with a cut-off frequency of 0.002 Hz (1/500 s^{-1}). The slow fluctuating component [V] is the band-passed signal with the upper and lower cut-off frequencies set at 0.33 Hz and 0.002 Hz (1/3 s^{-1} and 1/500 s^{-1} respectively). The turbulent component v is the high-pass filtered data with a cut-off frequency of 0.33 Hz (1/3 s^{-1}). Thus v is zero on average and v' is the standard deviation of the turbulent velocity component. A sensitivity analysis indicated that the low-pass filtered velocity <V> was little affected by a cut-off frequency below 0.002 to 0.005 Hz, while the fast fluctuating turbulent component v and its standard deviation v' were nearly independent of an upper cut-off frequency greater than 0.1 to 0.3 Hz.

All the statistical properties of turbulent velocity components were calculated over a 500 s interval (25,000 data samples). The same triple decomposition treatment was applied to the water depth, velocity flux and suspended sediment flux data. Lastly the relative ADV sensor depth z/d was z/d = 0.39, 0.12 and 0.32 at t = 72,000 s, 127,800 s and 145,800 s respectively.

MEAN FLOW PROPERTIES

The water level data presented a mean trend which was close to the Brisbane River record at the City Gauge (Fig. 3B). The present data provided, however, a greater level of details because of the high-temporal resolution. The water level fluctuations were significant. On average during the data series 1, the average deviation of instantaneous water level from the mean level was (h-<h>)' = 0.10 m. The large fluctuations were predominantly caused by relatively long-period oscillations with periods greater than 3 s. The standard deviation of the turbulent fluctuations (i.e. high-pass filtered data with 0.33 Hz cut-off) was significantly smaller: h' = 0.003 m on average for data series 1.

The velocity flux $q=V_xh$ corresponded to a longitudinal volume discharge per unit width defined in terms of the longitudinal velocity measured 0.35 m above the invert and the water level h recorded above the ADV pressure sensor. The field data showed large fluctuations of velocity flux around an almost constant trend. For the data set 1, $<q> = 0.25$ m^2/s on average with a deviation from mean flux $(q-<q>)' = 0.10$ m^2/s. For comparison, the standard deviation of turbulent flux fluctuations was significantly smaller: q' = 0.018 m^2/s on average. The relatively large, slow fluctuations in velocity flux were consistent with the personal observations by the investigators when they were standing in the floodwater.

The time-variations of velocity components are presented in Figure 6. Herein V_x is the longitudinal velocity positive downstream with its direction defined in Table 1 (column 8), V_y is the horizontal transverse velocity component, and V_z is the vertical velocity positive upwards. Each graph includes the instantaneous data V, the mean value $<V>$ and the standard deviation v' of the turbulent fluctuations. The data showed a slow decrease in longitudinal velocity magnitude during the data series 1 (location A) while the water level was increasing gently. The trend was unexpected but might be linked with some local geometry effects. During the receding flood (data series 2, location B), the velocity magnitude decreased with increasing time and declining water level. It was quantitatively comparable to the velocity magnitude in series 1 despite lower flood stage. The last data series 3 (location B) was conducted in very shallow waters with local water depth ranging from 0.26 m down to 0.10 m when the ADV receivers came out of the water. The velocity magnitude was then very small: $<V_x> \approx 0.002$ m/s on average for data series 3.

The transverse velocity data fluctuated around zero (Fig. 6B). The fluctuations were smaller than the fluctuations in longitudinal and vertical velocity components. On average, the standard deviation of transverse velocity fluctuations about the mean was 0.4 times the standard deviation of the longitudinal velocity fluctuations about the mean: i.e., $(V_y-<V_y>)'/(V_x-<V_x>)' \approx 0.4$. The lesser transverse velocity fluctuations seemed to be a feature of the flood flow motion because the same trend was observed at both locations with two different ADV settings and mountings.

The vertical velocity data were typically non-zero and positive, in particular at location A. For the data series 1, the ADV unit was positioned on a pylon above a small traffic island, resulting in a flow geometry comparable to a forward-facing step. It is thought that the island kerb induced a significant modification of the streamline pattern, possibly with formation of a recirculation bubble redirecting upwards the streamlines. The exact flow pattern was complicated by the skewed flow direction with the island kerb as well as by the presence of surrounding obstacles including an upstream structural column.

The velocity data indicated some unusual event during data series 2 about t = 136,000 to 140,000 s (Fig. 6B & 6). During this period, the mean flow direction shifted by up to 12º to the left when looking downstream (Fig. 7A). The relative transverse turbulent intensity v_y'/v_x' increased sharply as seen in Figure 7B, as a combination of a higher values in terms of v_y' and slightly lower values in terms of v_x' during the event. The same event was associated with a sharp increase in suspended sediment flux (see below). The exact causes of this unusual flow pattern are unknown, but its impact on the flow in Gardens Point Road was significant and clearly recorded.

VELOCITY FLUCTUATIONS

The velocity data indicated some large fluctuations around the mean values (Fig. 6). These included the slow fluctuating component and the turbulent motion. An assessment of the contribution of the slow fluctuations to the total turbulence intensity was made by applying the above decomposition to the original velocity signal. In the power spectrum density function data (e.g. Fig. 5B), the turbulence of the low-frequency side of the spectrum describes the slow fluctuations. The results show that the contribution of small-scale turbulence fluctuations was not significant and the slow-fluctuation turbulence intensity was nearly equal to the total (Fig. 8A). Henceforth the total turbulence intensity may be used as an indication of the combined effect of large-scale turbulence and sloshing.

The longitudinal turbulent intensity $v_x'/<V_x>$ was on average 5 to 6% for data series 1 and 2. Such a result was close to laboratory measurements in open channels although possibly slightly larger (Nezu and Nakagawa 1993, Xie 1998). The transverse and vertical relative turbulence intensities v_y'/v_x' and v_z'/v_x' showed some difference between locations A and B. On average for the data series 1 and 2, v_y'/v_x' was equal to 0.96 and 0.75 at z = 0.35 and 0.083 m respectively, and v_z'/v_x' equalled 1.14 and 0.83 at z = 0.35 and 0.083 m respectively. At z = 0.35 m, the results suggested that the turbulence was approximately isotropic: $v_x' \approx v_y' \approx v_z'$. At z = 0.083 m, the data indicated some anisotropy and the overall results tended to ratios v_y'/v_x' and v_z'/v_x' close to those observed in laboratory studies with straight prismatic rectangular channels (Nezu and Nakagawa 1993, Nezu 2005, Koch and Chanson 2009).

While the same data trend was observed for all velocity components (Fig. 8A showing V_x daya only), a different result was observed in terms of suspended sediment concentration (SSC). Through most data sets, the contribution of small-scale SSC fluctuations was significant and larger than the contribution of slow fluctuations when the SSC fluctuations were less than 1.5 kg/m^3: i.e., ssc'/SSC' ≈ 0.72 on average for all the data. For larger SSC fluctuations (i.e. SSC' > 1.5 kg/m^3), the slow-fluctuation turbulent term was nearly equal to the total fluctuations (Fig. 8B). The findings are summarised in Table 3, showing the median values of the turbulence intensity ratios [V]'/V' and v'/V' for all three velocity components, as well as the results in terms of the suspended sediment concentration SSC and suspended sediment flux $q_s = V_x SSC$ data.

SUSPENDED SEDIMENT FLUX

The time-variations of longitudinal suspended sediment flux $q_s = V_x SSC$ are presented in Figure 9 using the high concentration limb of the appropriate calibration curve shown in Figure 4. Herein q_s represents the sediment flux per unit area. The suspended sediment concentrations were calculated from the measured acoustic backscatter amplitude which was measured simultaneously with the longitudinal velocity V_x in the same sampling volume located 5 cm away from the ADV emitter. Figure 9 includes the instantaneous data, the mean value $<q_s>$ and the standard deviation q_s' of the turbulent fluctuation component. The Brisbane City Gauge data are shown for comparison.

The longitudinal suspended sediment flux data q_s showed some substantial flux values which would be consistent with the murky colour of the Brisbane River during the flood. The data highlighted a major increase in sediment flux about t = 136,263 s (Fig. 9). It is believed to be linked with high values of both SSC and velocity during a major flow episode (see above). During the data series 3, the data indicated some low sediment flux despite some large suspended sediment concentrations highlighted in Figure 7. This data series 3 corresponded to a period likely associated with suspended sediment deposition on the invert.

A statistical analysis suggested that most fluctuations in SSC were relatively rapid with periods less than 3 s. The results implied some differences in time scales between turbulent velocity and SSC fluctuations. The finding might suggest that the velocity fluctuations were linked with local effects and features of the urban environment, while the suspended sediment concentration and flux were affected predominantly by the sediment wash load.

It is worth to note that the last data series 3 took place in very shallow waters (less than 0.26 m). The turbulent velocity data showed a flow pattern markedly different from the other data series (Fig. 6). The very slow flow motion suggested that the flow in the car park was disconnected from the main river channel. The disconnection might be caused by the concrete blocks and traffic islands between the car park and Gardens Point and between Gardens Point Road and the river bank. An alternative might be the stoppage of the flow into the C Block building car park at the north-western end of the building.

CONCLUSION

During the January 2011 flood of the Brisbane River, some field measurements were conducted in an inundated urban environment on the river left bank. The turbulent velocity data were collected at relatively high frequency (50 Hz) using acoustic Doppler velocimetry in Gardens Point Road. The ADV signal amplitude was calibrated to give the suspended sediment concentration, thus providing the simultaneous measurements of three velocity components and suspended sediment flux in the same sampling volume with the same temporal resolution.

The field deployment showed some unusual features of flood flow in an urban environment. Namely the water elevations and velocities fluctuated with distinctive periods between 50 and 100 s. These slow fluctuations were linked with some local topographic effects: that is, some local choke induced by a constriction between stairwell cases located upstream of the sampling location. The high energy loss associated with choking would cause a flow re-direction around the stairwells and some slow oscillations with a period close to the natural sloshing period of the building car park length. The instantaneous velocity data were analysed using a triple decomposition. The same decomposition analysis was applied to the water depth, velocity flux and suspended sediment flux data. The velocity fluctuation data showed a large energy component in the slow fluctuation range, while the turbulent motion components were much smaller: $v'/(V-<V>)' \sim 0.1$. On the other hand, the high-frequency turbulent properties were comparable to turbulent characteristics observed in turbulent boundary layers and prismatic open channel flow configurations. The suspended sediment data highlighted some significant longitudinal flux. Both velocity and suspended sediment flux data showed a major event during the data series 2 which remains unexplained.

Lastly the third data set was collected in very shallow waters and it is suggested that the flow was disconnected from the main river channel. The turbulent properties were most likely affected by the interactions between suspended sediment deposition and flow turbulence.

This study shows that the triple decomposition approach originally developed for period flows may well be suited to complicated flood flows in an urban environment. Present results suggested that the high-frequency turbulence characteristics were similar to turbulence properties in canonical turbulent flows, and that the contribution of slow fluctuations was significant in terms of the overall turbulent kinetic energy.

ACKNOWLEDGEMENTS

The authors thank all people who participated in the field study, as well as those who assisted with the preparation and with the data analysis: without them, the study would not have been possible. The authors acknowledge some helpful discussions with Dr Frédérique Larrarte, Dr Mark Trevethan and Professor Laurent David. Lastly, the authors thank their respective families for their support during the difficult period of the flood in Brisbane.

REFERENCES

Asai, Y., Ishigaki, T., Baba, Y., and Toda, K. (2010). "Safety Analysis of Evacuation Routes Considering Elderly Persons during Underground Flooding." *Jl of Hydroscience and Hydraulic Eng.*, JSCE, Vol. 28, No. 2, pp. 15-21.

Bates, P.D., Horritt, M.S., Aronica, G., and Beve, K. (2004). "Bayesian Updating of Flood Inundation Likelihoods Conditioned on Flood Extent Data." *Hydrological Processes*, Vol. 18, No. 17, pp. 3347-3370.

Brown, R., Chanson, H., McIntosh, D., and Madhani, J. (2011). "Turbulent Velocity and Suspended Sediment Concentration Measurements in an Urban Environment of the Brisbane River Flood Plain at Gardens Point on 12-13 January 2011." *Hydraulic Model Report No. CH83/11*, School of Civil Engineering, The University of Queensland, Brisbane, Australia, 120 pages.

Chanson, H. (2011). "The 2010-2011 Floods in Queensland (Australia): Observations, First Comments and Personal Experience." *Journal La Houille Blanche*, No. 1, pp. 5-11.

Chanson, H., Reungoat, D., Simon, B., and Lubon, P. (2012). "High-Frequency Turbulence and Suspended Sediment Concentration Measurements in the Garonne River Tidal Bore." *Estuarine Coastal and Shelf Science*, (DOI 10.1016/j.ecss.2011.09.012) (On-line first).

Fox, J.F., Papanicolaou, A.N., and Kjos, L. (2005). "Eddy Taxonomy Methodology around Submerged Barb Obstacle within a Fixed Rough Bed." *Jl of Eng. Mech.*, ASCE, Vol. 131, No. 10, pp. 1082-1101.

Goring, D.G., and Nikora, V.I. (2002). "Despiking Acoustic Doppler Velocimeter Data." *Jl of Hyd. Engrg.*, ASCE, Vol. 128, No. 1, pp. 117-126. Discussion: Vol. 129, No. 6, pp. 484-489.

Ha, H.K., Hsu, W.Y., Maa, J.P.Y., Shao, Y.Y., and Holland, C.W. (2009). "Using ADV Backscatter Strength for Measuring Suspended Cohesive Sediment Concentration." *Continental Shelf Research*, Vol. 29, pp. 1310-1316.

Henderson, F.M. (1966). "Open Channel Flow." *MacMillan Company*, New York, USA.

Hussain, A.K.M.F., and Reynolds, W.C. (1972). "The Mechanics of on Organized Wave in Turbulent Shear Flow. Part 2: Experimental Results." *Jl of Fluid Mech.*, Vol. 54, Part 2, pp. 241-261.

Institution of Engineers, Australia (1974). "Proceedings of Symposium January 1974 Floods Moreton Region." *The Institution of Engineers, Australia*, Queensland Division, F. Cossins and G. Heatherwick Editors, Aug., 275 pages.

Ishigaki, T., Keiichi, T., and Kazuya, I. (2003). "Hydraulic Model Tests of Inundation in Urban Area with Underground Space." *Proc. 30th IAHR Biennial Congress*, Thessaloniki, Greece, Vol. B, p. 487-493.

Koch, C., and Chanson, H. (2009). "Turbulence Measurements in Positive Surges and Bores." *Journal of Hydraulic Research*, IAHR, Vol. 47, No. 1, pp. 29-40 (DOI: 10.3826/jhr.2009.2954).

McLelland, S.J., and Nicholas, A.P. (2000). "A New Method for Evaluating Errors in High-Frequency ADV Measurements." *Hydrological Processes*, Vol. 14, pp. 351-366.

Montes, J.S. (1998). "Hydraulics of Open Channel Flow." *ASCE Press*, New-York, USA, 697 pages.

Nania, L., Gomez, M., and Dolz, J. (2004). "Experimental Study of the Dividing Flow in Steep Street Crossings." *Jl of Hyd. Res.*, IAHR, Vol. 42, No. 4, pp. 406-412.

Nezu, I. (2005). "Open-Channel Flow Turbulence and its Research Prospect in the 21st Century." *Jl of Hyd. Engrg.*, ASCE, Vol. 131, No. 4, pp. 229-246.

Nezu, I., and Nakagawa, H. (1993). "Turbulence in Open-Channel Flows." *IAHR Monograph*, IAHR Fluid Mechanics Section, Balkema Publ., Rotterdam, The Netherlands, 281 pages.

Solo-Gabriele, H.M., and Perkins, F.E. (1997). "Streamflow and Suspended Sediment Transport in an Urban Environment." *Jl of Hyd. Engrg.*, ASCE, Vol. 123, No. 9, pp. 807-811

Thieken, A.H., Muller, M., Kreibich, H., and Merz, B. (2005). "Flood Damage and Influencing Factors: New Insights from the August 2002 Flood in Germany." *Water Res. Res.*, AGU, Vol. 41, No. 12, Paper W12430 (DOI: 10.1029/2005WR004177).

Velickovic, M., Soares-Frazao, S., and Zech, Y. (2011). "Porosity Model of Flow through an Idealised Urban District. Influence of City Alignment and of Transient Flow Character." *Proc. 34th IAHR World Congress*, Brisbane, Australia, 26 June-1 July, Engineers Australia Publication, Eric Valentine, Colin Apelt, James Ball, Hubert Chanson, Ron Cox, Rob Ettema, George Kuczera, Martin Lambert, Bruce Melville and Jane Sargison Editors, pp. 3823-3830.

Wahl, T.L. (2003). "Despiking Acoustic Doppler Velocimeter Data. Discussion." *Jl of Hyd. Engrg.*, ASCE, Vol. 129, No. 6, pp. 484-487.

Werner, M.G.F., Hunter, N.M., and Bates, P.D. (2005). "Identifiability of Distributed Floodplain Roughness Values in Flood Extent Estimation." *Jl of Hydrology*, Vol. 314, No. 1-4, pp. 139-157.

Xie, Q. (1998). "Turbulent Flows in Non-Uniform Open Channels: Experimental Measurements and Numerical Modelling." *Ph.D. thesis*, Dept. of Civil Eng., University Of Queensland, Australia, 339 pages.

Yossef, M.F.M., and Vriend, H.J. de (2011). "Flow Details near River Groynes: Experimental Investigation." *Jl of Hyd. Engrg.*, ASCE, Vol. 137, No. 5, pp. 504-516.

NOTATION

d	water depth (m);
d_{50}	median grain size (m) defined as the size for which 50% by weight of the material is finer;
h	instantaneous pressure head (m), or water level, measured above the ADV pressure sensor;
q	instantaneous longitudinal velocity flux (m^2/s): $q = V_x h$;
q_s	instantaneous longitudinal suspended sediment flux (kg/s/m^2): $q_s = V_x SSC$;
SSC	instantaneous suspended sediment concentration (kg/m^3);
SSC'	standard deviation of suspended sediment concentration (kg/m^3);
ssc	turbulent suspended sediment concentration fluctuation (kg/m^3);
t	time (s);
V	instantaneous velocity (m/s): $V = \langle V \rangle + [V] + v$;
V'	standard deviation of the measured velocity (m/s);
V_x	instantaneous longitudinal velocity component (m/s);
V_x'	standard deviation of the longitudinal velocity component (m/s);
V_y	instantaneous transverse velocity component (m/s);
V_z	instantaneous vertical velocity component (m/s);
$\langle V \rangle$	mean velocity (m/s) calculated as low-pass filtered data with a cut-off frequency of 0.002 Hz (1/500 s^{-1});
$[V]$	slow fluctuating velocity (m/s) calculated as the band-passed signal with the upper and lower cut-off frequencies set at 0.33 Hz and 0.002 Hz (1/3 s^{-1} and 1/500 s^{-1} respectively);
$[V]'$	standard deviation of the slow fluctuating velocity component(m/s);
v	turbulent velocity fluctuation (m/s): $v = V - \langle V \rangle - [V]$; v is the high-pass filtered data with a cut-off frequency of 0.33 Hz (1/3 s^{-1});
v'	standard deviation of the turbulent velocity fluctuation (m/s) calculated over 500 s;
v_x'	standard deviation of the longitudinal turbulent velocity fluctuation (m/s) calculated over 500 s;
v_y'	standard deviation of the transverse turbulent velocity fluctuation (m/s) calculated over 500 s;
v_z'	standard deviation of the vertical turbulent velocity fluctuation (m/s) calculated over 500 s;

Subscript

x	longitudinal direction positive downstream;
y	transverse direction positive towards the left;
z	vertical direction positive upwards;

Abbreviations

ADV acoustic Doppler velocimeter;

AHD Australian Height Datum (or Mean Sea Level);

Note

All times are expressed in local Queensland time (GMT + 10).

BROWN, R, and CHANSON, H. (2013). "Turbulence and Suspended Sediment Measurements in an Urban Environment during the Brisbane River Flood of January 2011." *Journal of Hydraulic Engineering*, ASCE, Vol. 139, No. 2, pp. 244-252 (DOI: 10.1061/(ASCE)HY.1943-7900.0000666) (ISSN 0733-9429).

Table 1 - Turbulent velocity measurements in Gardens Point Road during the 2011 Brisbane River flood

Data set (1)	ADV location (2)	Sampling rate Hz (3)	Velocity range m/s (4)	Start time (5)	Duration (6)	z m (7)	Flow direction (8)
1	A	50	2.5	12/01/2011 at 20:40:08	4 h 26 min 40 s	0.350	160.8º
2	B	50	1.0	13/01/2011 at 12:08:55	3 h 48 min 38 s	0.083	172.2º
3	B	50	1.0	13/01/2011 at 17:34:40	1 h 5 min 35 s	0.083	172.2º

Notes: Location A: ADV unit mounted horizontally on boom gate support; Location B: ADV unit mounted vertically on a hand rail; Flow direction: mean longitudinal flow direction at the sampling location relative to the geographic north; z: ADV sampling volume elevation above the invert.

Table 2 - Dominant period(s) of the slow fluctuations during the field study in the inundated Gardens Point Road on 12-13 January 2011

Data set	Period (s)						
(1)	h (2)	$q=h\times V_x$ (3)	V_x (4)	V_y (5)	V_z (6)	SSC (7)	$q_s=SSC\times V_x$ (8)
1	58	57	57	56	57	56	57
2	--	--	88	92	89	N/A	73 & 101
3	--	--	101	105	59 & 101	61	134

Table 3 - Median relative contribution of the slow fluctuations and turbulent motion on the total turbulence intensity in Gardens Point Road during the Brisbane River flood on 12-13 January 2011

Data set (1)	z m (2)	$[V_x]'/V_x'$ median (3)	v_x'/V_x' median (4)	$[V_y]'/V_y'$ median (5)	v_y'/V_y' median (6)	$[V_z]'/V_z'$ median (7)	v_z'/V_z' median (8)	[SSC]' /SSC' median (9)	ssc' /SSC' median (10)	$[q_s]'/(q_s)$. median (11)	$q_s'/(q_s)'$ median (12)
1	0.350	0.94	0.37	0.69	0.58	0.95	0.23	0.31	0.93	0.88	0.43
2	0.083	0.90	0.29	0.50	0.73	0.94	0.24	0.83	0.48	0.89	0.32
3	0.083	0.93	0.29	0.47	0.79	0.95	0.20	0.62	0.76	0.94	0.28

Notes: median over the data set duration; standard deviations calculated over 500s.

BROWN, R, and CHANSON, H. (2013). "Turbulence and Suspended Sediment Measurements in an Urban Environment during the Brisbane River Flood of January 2011." *Journal of Hydraulic Engineering*, ASCE, Vol. 139, No. 2, pp. 244-252 (DOI: 10.1061/(ASCE)HY.1943-7900.0000666) (ISSN 0733-9429).

LIST OF CAPTIONS

Fig. 1 - Photographs of the investigation site prior to the flood

(A) Aerial view of Brisbane's Central Business District in 2007 looking North (Copyright the University of Queensland) - The Brisbane River flows from left to right - The ADV sampling site is highlighted with the red arrow

(B) Aerial view of Gardens Point Road and C Block building in 2001 (Copyright Queensland University of Technology) - The ADV sampling site is highlighted with the red arrow

Fig. 2 - Investigation site during the flood

(A) Flooded Gardens Points Road and submerged ADV unit on 13 January 2011 at 11:40 during the flood - Blacks arrows show the main flow directions

(B) CAD drawing of the C Bock submerged car park - Blue arrows indicate the main flow direction - Note the constriction induced by the stairwells

(C) Surveyed cross-section of the left flood plain of the Brisbane River at Gardens Point looking downstream (South-East) - The red arrow marks the ADV location

Fig. 3 -Water level observations at the City Gauge (Port Office) and in Gardens Point Road

(A) Brisbane City Gauge data and predicted water elevations at the Port Office, and water depth observations at Gardens Point Road - The City Gauge data and observations at Gardens Point are reported in m AHD (Australian Height Datum)

(B) Instantaneous pressure head h measured above the ADV pressure sensor - Comparison with the City Gauge data and water surface observations at Gardens Point (in m AHD)

Fig. 4 - Relationship between ADV signal amplitude and suspended sediment concentration for both ADV velocity settings

Fig. 5 - Energy density spectra of water levels h, longitudinal velocity V_x and velocity flux $q = V_x h$ during the data series 1

(A, Left) Energy density spectrum of water levels h

(B, Right) Energy density spectrum of longitudinal velocity V_x

(C) Energy density spectrum of velocity flux $q = V_x h$

Fig. 6 - Time variations of the velocity components: instantaneous velocity V, mean velocity <V> and standard deviation v' of turbulent fluctuation component - Comparison with observed water elevations

(A) Longitudinal velocity component V_x

(B) Transverse velocity component V_y

(C) Vertical velocity component V_z

BROWN, R, and CHANSON, H. (2013). "Turbulence and Suspended Sediment Measurements in an Urban Environment during the Brisbane River Flood of January 2011." *Journal of Hydraulic Engineering*, ASCE, Vol. 139, No. 2, pp. 244-252 (DOI: 10.1061/(ASCE)HY.1943-7900.0000666) (ISSN 0733-9429).

Fig. 7 - Longitudinal and transverse velocity components during the data set #2

(A, Left) Horizontal velocity direction

(B, Right) Longitudinal velocity component and dimensionless ratio v_y'/v_x'

Fig. 8 - Comparison of the standard deviation of the measured data (V_x', SSC') to the slow-fluctuating and small-scale turbulent intensities ($[V_x]'$, [SSC]' & v_x', ssc') (standard deviations calculated every 60 s)

(A) Longitudinal velocity component V_x

(B) -Suspended sediment concentration SSC (Note logarithmic scales of axes)

Fig. 9 - Time variations of the longitudinal suspended sediment flux $q_s = V_x SSC$: instantaneous suspended sediment flux, mean suspended sediment flux $<V_x SSC>$ and standard deviation $(v_x ssc)'$ of the turbulent fluctuation component - Comparison with the Brisbane River City Gauge data reported in m AHD

BROWN, R, and CHANSON, H. (2013). "Turbulence and Suspended Sediment Measurements in an Urban Environment during the Brisbane River Flood of January 2011." *Journal of Hydraulic Engineering*, ASCE, Vol. 139, No. 2, pp. 244-252 (DOI: 10.1061/(ASCE)HY.1943-7900.0000666) (ISSN 0733-9429).

Fig. 1 - Photographs of the investigation site prior to the flood

(A) Aerial view of Brisbane's Central Business District in 2007 looking North (Copyright the University of Queensland) - The Brisbane River flows from left to right - The ADV sampling site is highlighted with the red arrow

BROWN, R, and CHANSON, H. (2013). "Turbulence and Suspended Sediment Measurements in an Urban Environment during the Brisbane River Flood of January 2011." *Journal of Hydraulic Engineering*, ASCE, Vol. 139, No. 2, pp. 244-252 (DOI: 10.1061/(ASCE)HY.1943-7900.0000666) (ISSN 0733-9429).

(B) Aerial view of Gardens Point Road and C Block building in 2001 (Copyright Queensland University of Technology) - The ADV sampling site is highlighted with the red arrow

BROWN, R, and CHANSON, H. (2013). "Turbulence and Suspended Sediment Measurements in an Urban Environment during the Brisbane River Flood of January 2011." *Journal of Hydraulic Engineering*, ASCE, Vol. 139, No. 2, pp. 244-252 (DOI: 10.1061/(ASCE)HY.1943-7900.0000666) (ISSN 0733-9429).

Fig. 2 - Investigation site during the flood

(A) Flooded Gardens Points Road and submerged ADV unit on 13 January 2011 at 11:40 during the flood - Blacks arrows show the main flow directions

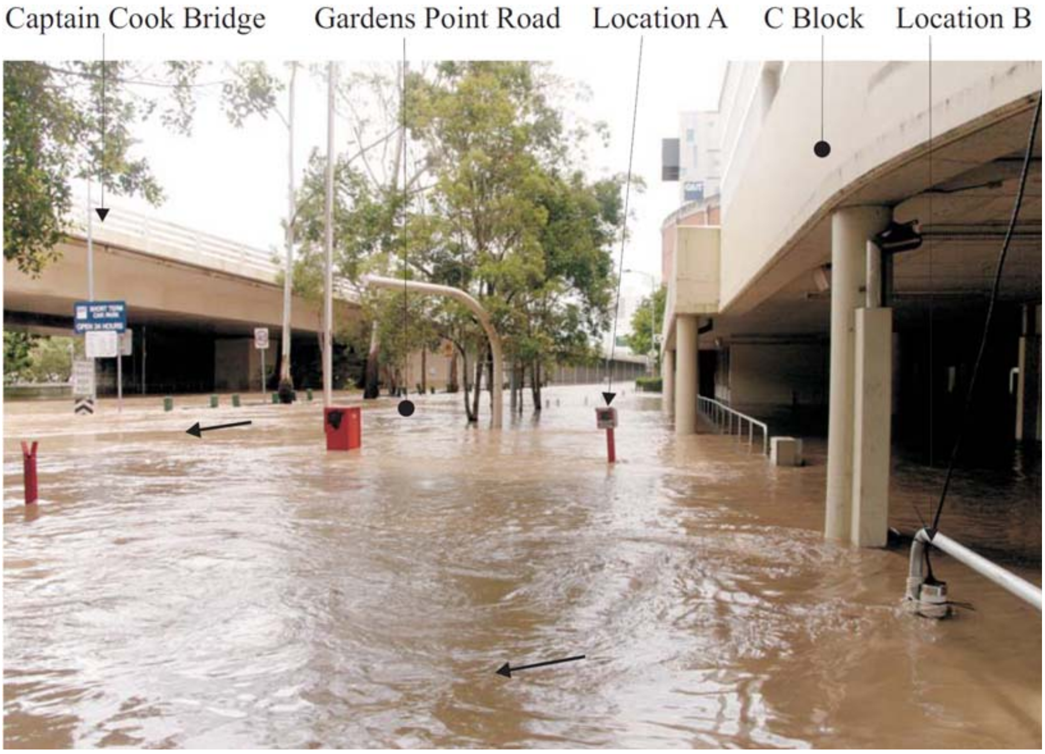

(B) CAD drawing of the C Bock submerged car park - Blue arrows indicate the main flow direction - Note the constriction induced by the stairwells

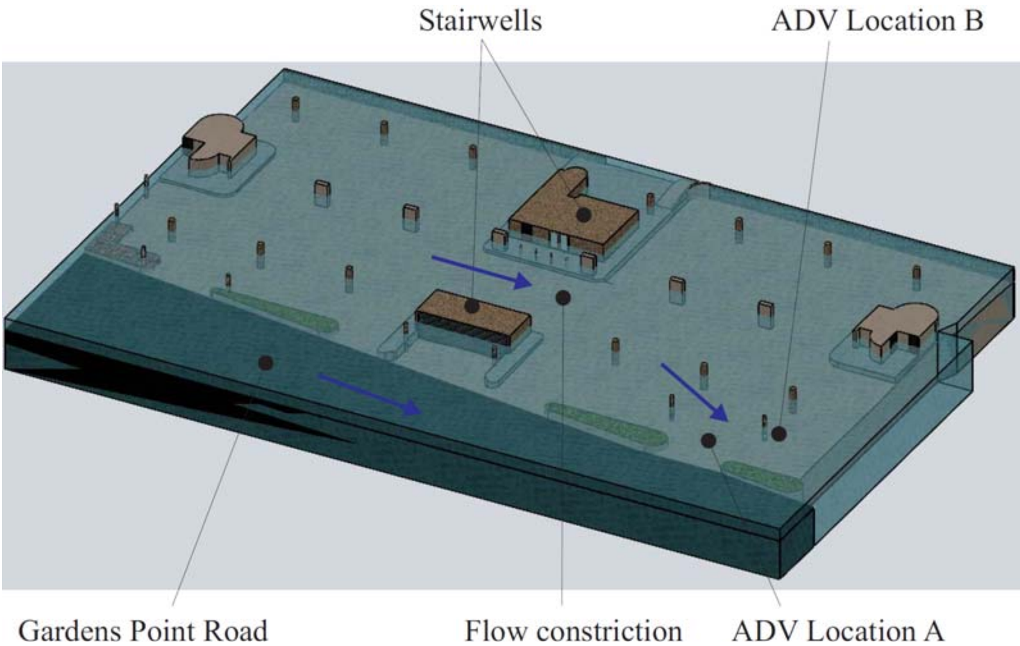

BROWN, R, and CHANSON, H. (2013). "Turbulence and Suspended Sediment Measurements in an Urban Environment during the Brisbane River Flood of January 2011." *Journal of Hydraulic Engineering*, ASCE, Vol. 139, No. 2, pp. 244-252 (DOI: 10.1061/(ASCE)HY.1943-7900.0000666) (ISSN 0733-9429).

(C) Surveyed cross-section of the left flood plain of the Brisbane River at Gardens Point looking downstream (South-East) - The red arrow marks the ADV location

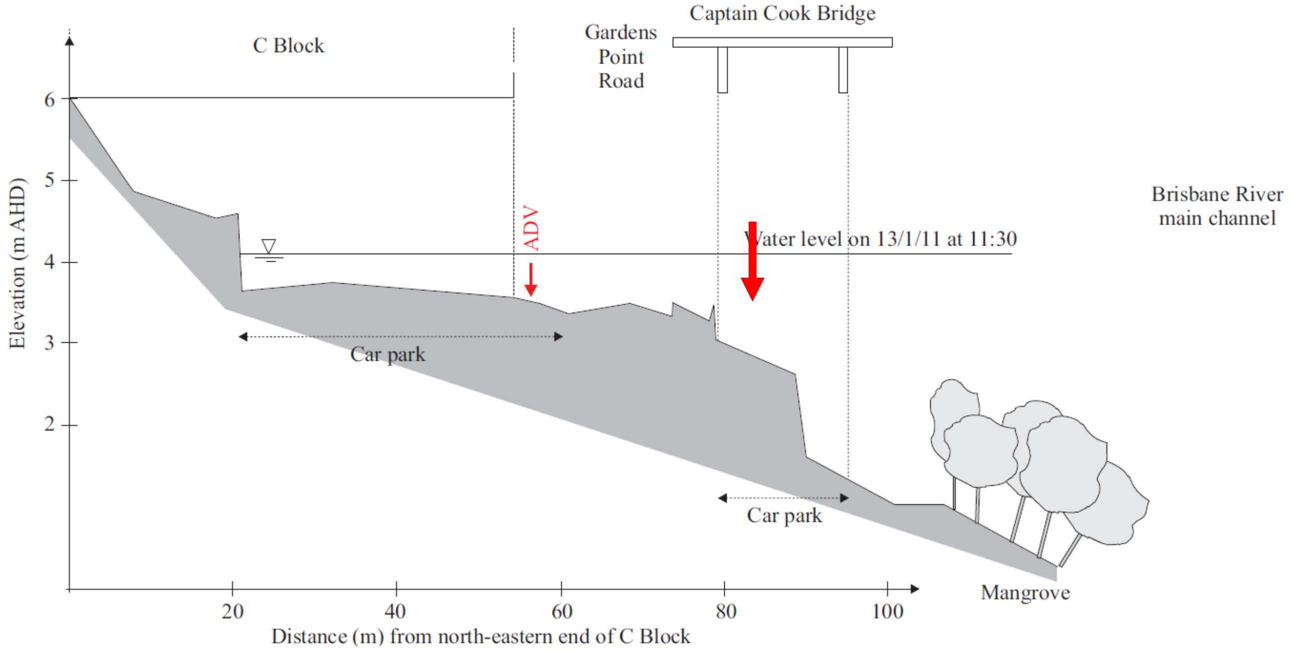

BROWN, R, and CHANSON, H. (2013). "Turbulence and Suspended Sediment Measurements in an Urban Environment during the Brisbane River Flood of January 2011." *Journal of Hydraulic Engineering*, ASCE, Vol. 139, No. 2, pp. 244-252 (DOI: 10.1061/(ASCE)HY.1943-7900.0000666) (ISSN 0733-9429).

Fig. 3 -Water level observations at the City Gauge (Port Office) and in Gardens Point Road

(A) Brisbane City Gauge data and predicted water elevations at the Port Office, and water depth observations at Gardens Point Road - The City Gauge data and observations at Gardens Point are reported in m AHD (Australian Height Datum)

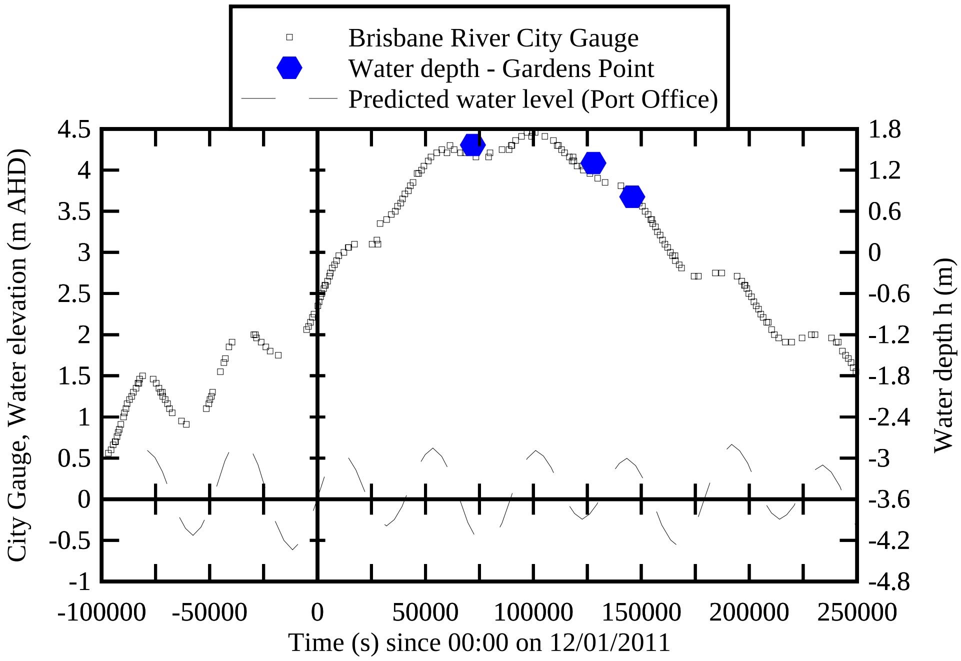

(B) Instantaneous pressure head h measured above the ADV pressure sensor - Comparison with the City Gauge data and water surface observations at Gardens Point (in m AHD)

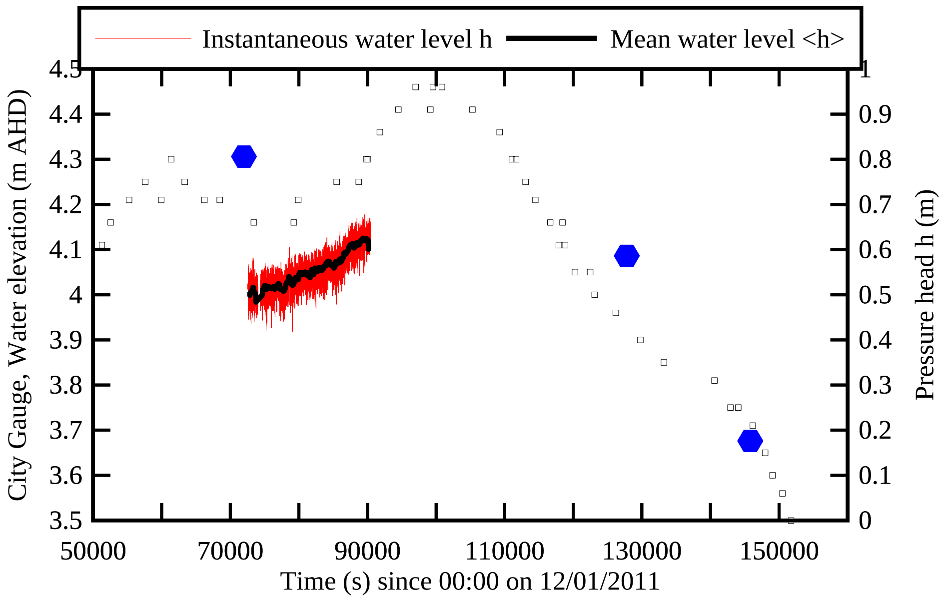

BROWN, R, and CHANSON, H. (2013). "Turbulence and Suspended Sediment Measurements in an Urban Environment during the Brisbane River Flood of January 2011." *Journal of Hydraulic Engineering*, ASCE, Vol. 139, No. 2, pp. 244-252 (DOI: 10.1061/(ASCE)HY.1943-7900.0000666) (ISSN 0733-9429).

Fig. 4 - Relationship between ADV signal amplitude and suspended sediment concentration for both ADV velocity settings

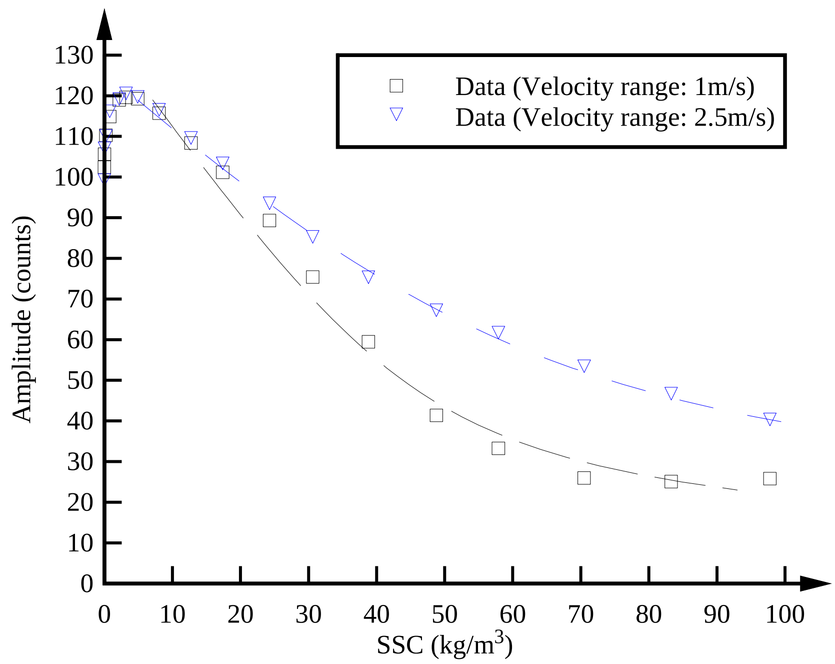

BROWN, R, and CHANSON, H. (2013). "Turbulence and Suspended Sediment Measurements in an Urban Environment during the Brisbane River Flood of January 2011." *Journal of Hydraulic Engineering*, ASCE, Vol. 139, No. 2, pp. 244-252 (DOI: 10.1061/(ASCE)HY.1943-7900.0000666) (ISSN 0733-9429).

Fig. 5 - Energy density spectra of water levels h, longitudinal velocity V_x and velocity flux $q = V_x h$ during the data series 1

(A, Left) Energy density spectrum of water levels h

(B, Right) Energy density spectrum of longitudinal velocity V_x

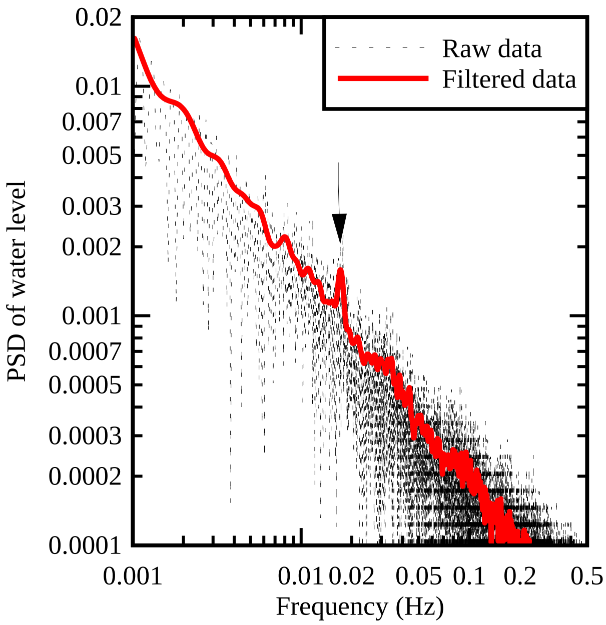

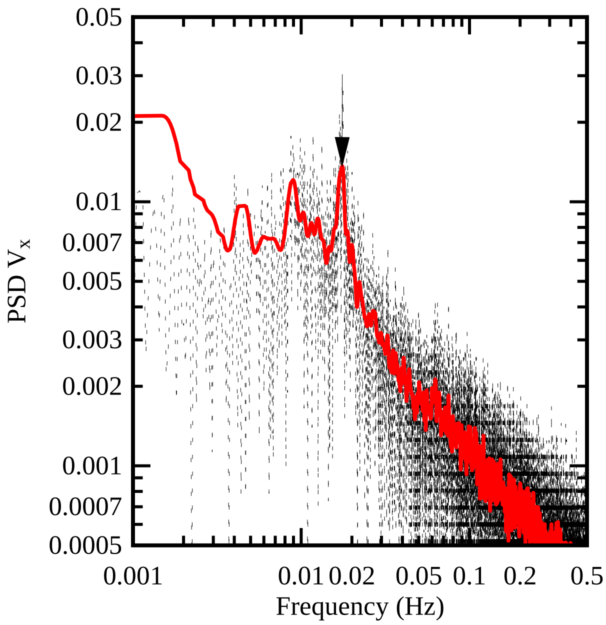

(C) Energy density spectrum of velocity flux $q = V_x h$

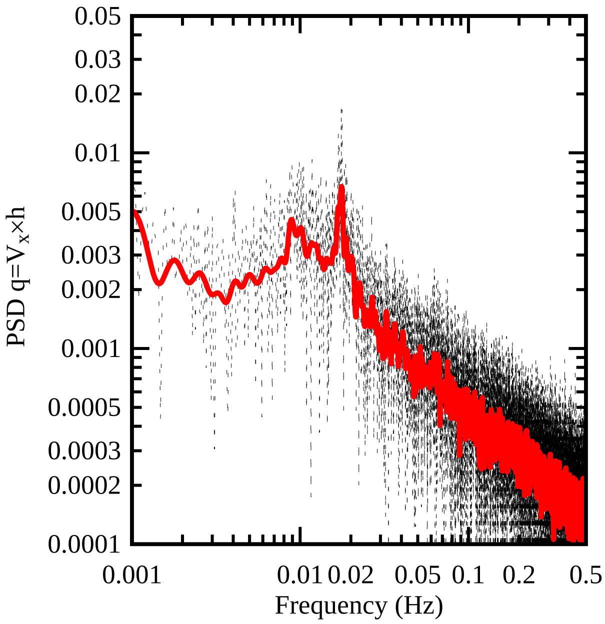

BROWN, R, and CHANSON, H. (2013). "Turbulence and Suspended Sediment Measurements in an Urban Environment during the Brisbane River Flood of January 2011." *Journal of Hydraulic Engineering*, ASCE, Vol. 139, No. 2, pp. 244-252 (DOI: 10.1061/(ASCE)HY.1943-7900.0000666) (ISSN 0733-9429).

Fig. 6 - Time variations of the velocity components: instantaneous velocity V, mean velocity <V> and standard deviation v' of turbulent fluctuation component - Comparison with observed water elevations

(A) Longitudinal velocity component V_x

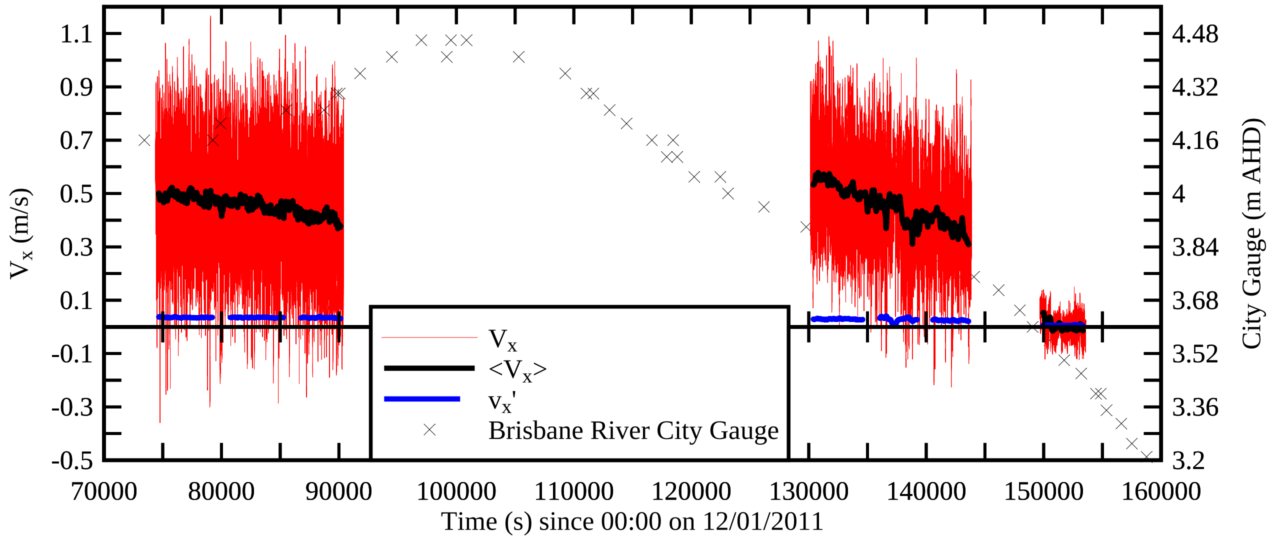

(B) Transverse velocity component V_y

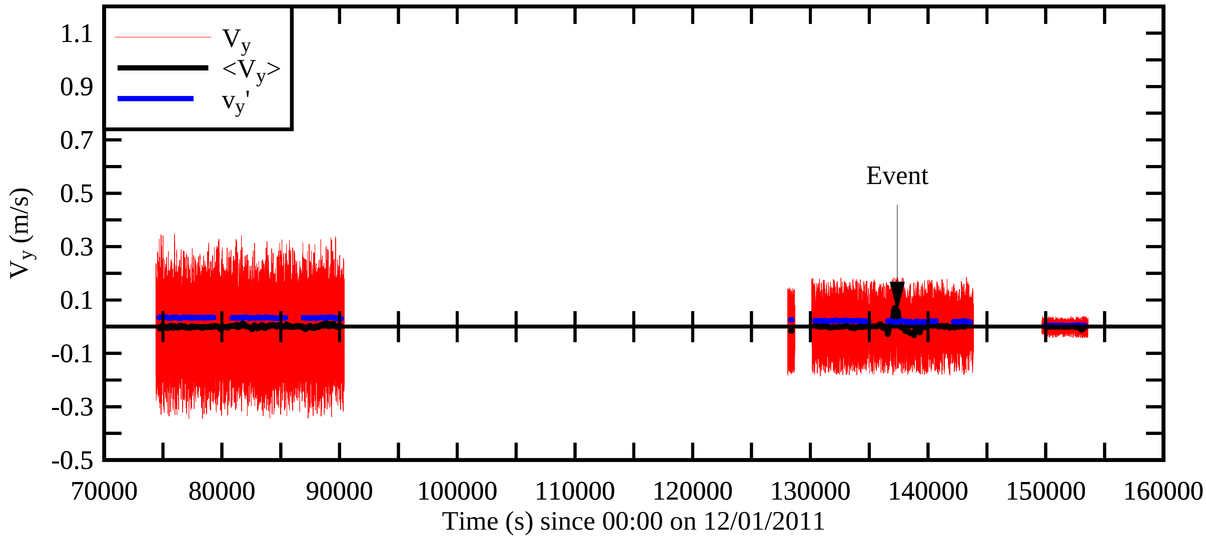

BROWN, R, and CHANSON, H. (2013). "Turbulence and Suspended Sediment Measurements in an Urban Environment during the Brisbane River Flood of January 2011." *Journal of Hydraulic Engineering*, ASCE, Vol. 139, No. 2, pp. 244-252 (DOI: 10.1061/(ASCE)HY.1943-7900.0000666) (ISSN 0733-9429).

(C) Vertical velocity component V_z

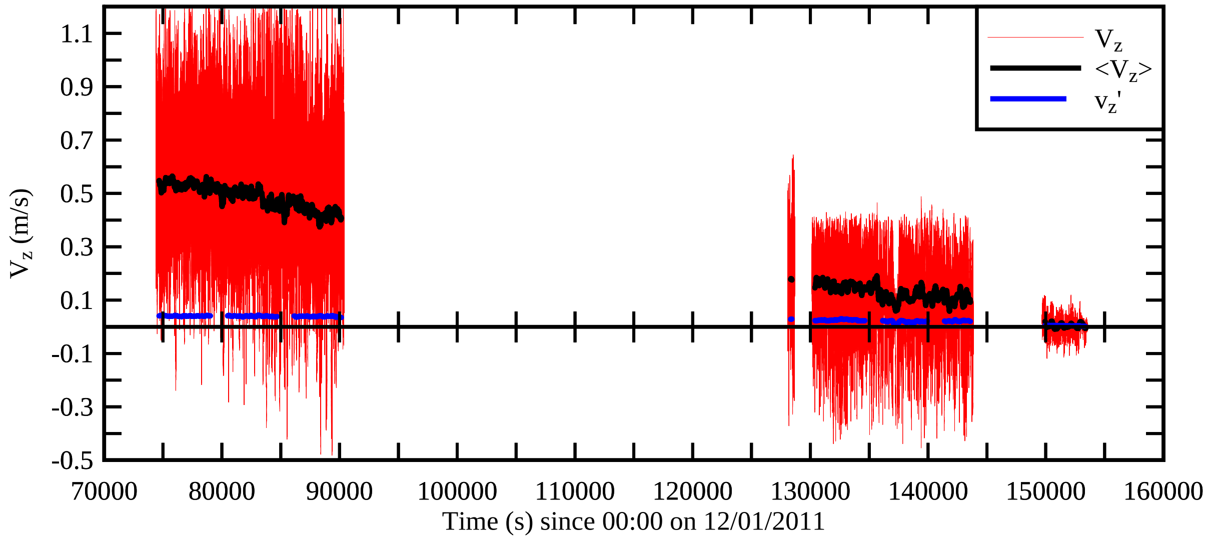

BROWN, R, and CHANSON, H. (2013). "Turbulence and Suspended Sediment Measurements in an Urban Environment during the Brisbane River Flood of January 2011." *Journal of Hydraulic Engineering*, ASCE, Vol. 139, No. 2, pp. 244-252 (DOI: 10.1061/(ASCE)HY.1943-7900.0000666) (ISSN 0733-9429).

Fig. 7 - Longitudinal and transverse velocity components during the data set #2

(A, Left) Horizontal velocity direction

(B, Right) Longitudinal velocity component and dimensionless ratio v_y'/v_x'

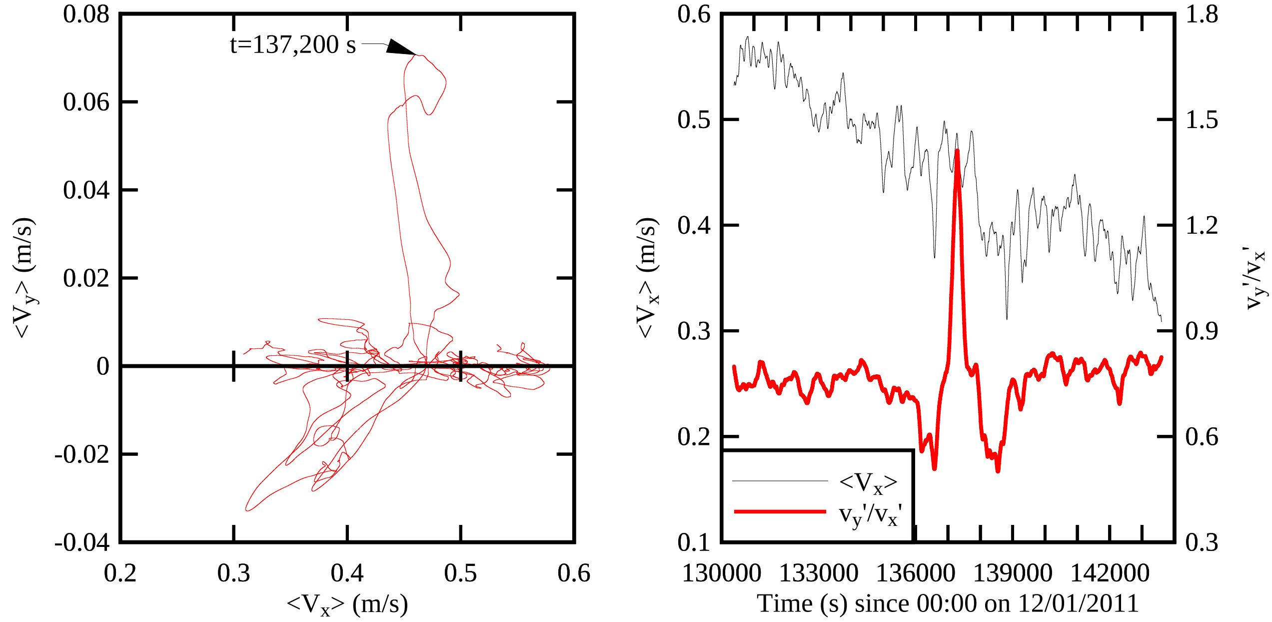

Fig. 8 - Comparison of the standard deviation of the measured data (V_x', SSC') to the slow-fluctuating and small-scale turbulent intensities ([V_x]', [SSC]' & v_x', ssc') (standard deviations calculated every 60 s)

(A) Longitudinal velocity component V_x

(B) -Suspended sediment concentration SSC (Note logarithmic scales of axes)

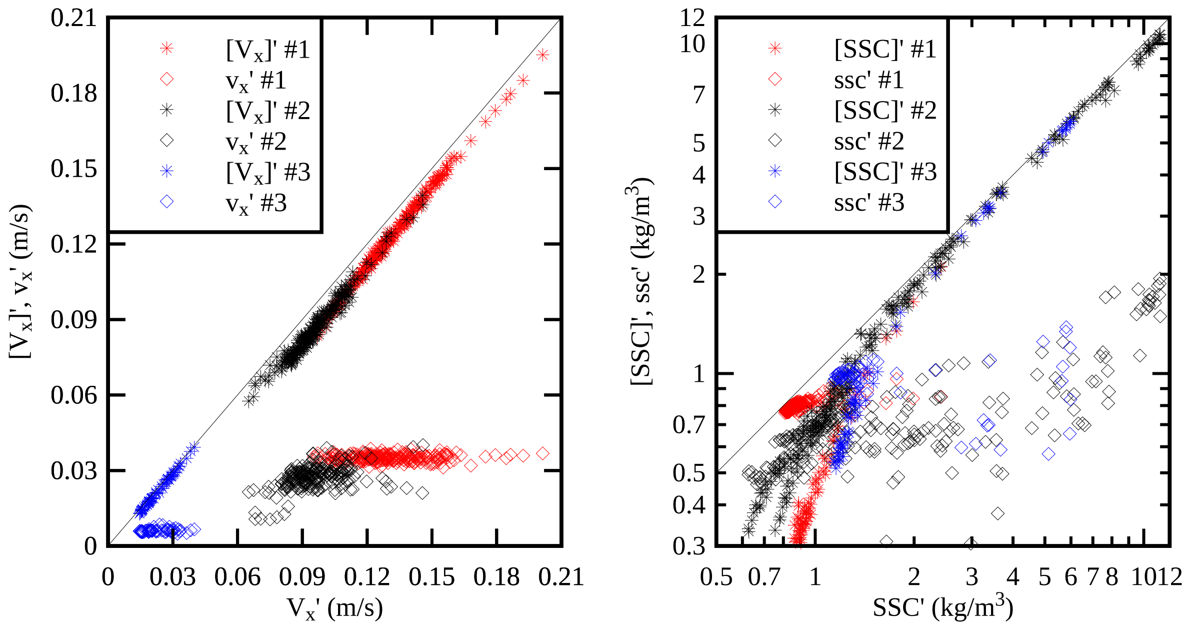

BROWN, R, and CHANSON, H. (2013). "Turbulence and Suspended Sediment Measurements in an Urban Environment during the Brisbane River Flood of January 2011." *Journal of Hydraulic Engineering*, ASCE, Vol. 139, No. 2, pp. 244-252 (DOI: 10.1061/(ASCE)HY.1943-7900.0000666) (ISSN 0733-9429).

Fig. 9 - Time variations of the longitudinal suspended sediment flux $q_s = V_xSSC$: instantaneous suspended sediment flux, mean suspended sediment flux $<V_xSSC>$ and standard deviation $(v_xssc)'$ of the turbulent fluctuation component - Comparison with the Brisbane River City Gauge data reported in m AHD